Investigation of the ATP Binding Site of *Escherichia coli* Aminoimidazole Ribonucleotide Synthetase Using Affinity Labeling and Site-Directed Mutagenesis†

E. J. Mueller,‡ S. Oh,‡ E. Kavalerchik,‡ T. J. Kappock,‡ E. Meyer,‡ C. Li,§ S. E. Ealick,*,§ and J. Stubbe*,‡

Departments of Chemistry and Biology, Massachusetts Institute of Technology, Cambridge, Massachusetts 02139, and Department of Chemistry and Chemical Biology, Cornell University, Ithaca, New York 14853

Received March 18, 1999; Revised Manuscript Received May 26, 1999

ABSTRACT: Aminoimidazole ribonucleotide (AIR) synthetase (PurM) catalyzes the conversion of formylglycinamide ribonucleotide (FGAM) and ATP to AIR, ADP, and P_i, the fifth step in de novo purine biosynthesis. The ATP binding domain of the *E. coli* enzyme has been investigated using the affinity label [^{14}C]-*p*-fluorosulfonylbenzoyl adenosine (FSBA). This compound results in time-dependent inactivation of the enzyme which is accelerated by the presence of FGAM, and gives a $K_i = 25\ \mu$M and a $k_{inact} = 5.6 \times 10^{-2}$ min^{-1}. The inactivation is inhibited by ADP and is stoichiometric with respect to AIR synthetase. After trypsin digestion of the labeled enzyme, a single labeled peptide has been isolated, I-X-G-V-V-K, where X is Lys27 modified by FSBA. Site-directed mutants of AIR synthetase were prepared in which this Lys27 was replaced with a Gln, a Leu, and an Arg and the kinetic parameters of the mutant proteins were measured. All three mutants gave k_{cat}s similar to the wild-type enzyme and K_ms for ATP less than that determined for the wild-type enzyme. Efforts to inactivate the chicken liver trifunctional AIR synthetase with FSBA were unsuccessful, despite the presence of a Lys27 equivalent. The role of Lys27 in ATP binding appears to be associated with the methylene linker rather than its ϵ-amino group. The specific labeling of the active site by FSBA has helped to define the active site in the recently determined structure of AIR synthetase [Li, C., Kappock, T. J., Stubbe, J., Weaver, T. M., and Ealick, S. E. (1999) *Structure* (in press)], and suggests additional flexibility in the ATP binding region.

Aminoimidazole ribonucleotide (AIR)[1] synthetase (PurM) catalyzes the fifth step of de novo purine biosynthesis: conversion of ATP and formylglycinamide ribonucleotide (FGAM) to AIR, ADP, and P_i (eq 1). The mechanism has

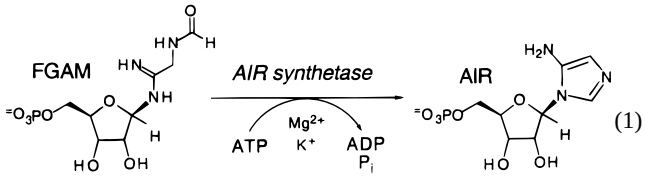

(1)

been proposed to involve an O-phosphorylated amide intermediate, which after attack by the N1 of the amidine of FGAM forms a five-membered ring that can lose both phosphate and a proton to generate AIR (*1*). A similar mechanism, using ATP to enhance the dehydration of amides, has been proposed for FGAM synthetase (PurL) (*2*), the fourth step in purine biosynthesis, and for cytidine triphosphate (CTP) synthetase, a key enzyme in pyrimidine biosynthesis (*3*). The structure of the *Escherichia coli* AIR synthetase in the absence of ligands has recently been solved (PDB id 1CLI) and represents a new class of ATP binding protein (*4*). Our recent sequence alignments between PurMs and a subclass of the PurLs suggest that they may belong to a new superfamily of ATP-requiring enzymes catalyzing similar chemical reactions. This paper describes our efforts, using affinity labeling and site-directed mutagenesis, to define the ATP binding domain of *E. coli* AIR synthetase. Identification of a single labeled peptide provides a starting point for our interpretation of our structural data.

A number of ATP affinity labels have been synthesized and used to identify residues within ATP binding domains (*5*, *6*). Fluorosulfonylbenzoyl adenosine (FSBA, Chart 1) can modify several nucleophilic amino acids, yielding protein adducts of differing chemical stability. However, only in the case of Lys (*7*) and Tyr (*8*) have the adducts of FSBA been sufficiently stable to allow isolation and identification of modified peptides. Other nucleophilic amino acid residues (Arg, His, Cys, and Ser) have been implicated in reaction with FSBA based on chemical reactivity studies, but the adducts have not been isolable (*9*−*12*). FSBA has thus proven itself to be a useful reagent in the identification of a variety of amino acids implicated in ATP binding.

† This work was supported by NIH Grant GM32191. T.J.K. was supported by NIH Cancer Training Grant CA09112.

* Authors to whom correspondence should be addressed. E-mail: stubbe@mit.edu or see3@cornell.edu.

‡ Massachusetts Institute Technology.

§ Cornell University.

[1] Abbreviations: AIR, aminoimidazole ribonucleotide; FGAM, formylglycinamide ribonucleotide; AIR synthetase, PurM; FGAM synthetase, PurL; FSBA, fluorosulfonylbenzoyl adenosine; LDH, lactate dehydrogenase; PK, pyruvate kinase; PEP, phosphoenolpyruvate; NADH, reduced β-nicotinamide adenine dinucleotide phosphate; BSA, bovine serum albumin; ATP, adenosine 5′-triphosphate; DTT, dithiothreitol; SDS−PAGE, sodium dodecyl sulfate−polyacrylamide gel electrophoresis; PTH, phenylthiohydantoin; TAE, Tris−acetate EDTA; TBE, Tris−borate EDTA; TFA, trifluoroacetic acid; TEA·OAc, triethylammonium acetate; IPTG, isopropyl β-D-thiogalactopyranoside; ss DNA, single-stranded DNA; ds DNA, double-stranded DNA; wt, wild-type; nd, not determined.

10.1021/bi990638r CCC: $18.00
Published on Web 07/13/1999

Chart 1

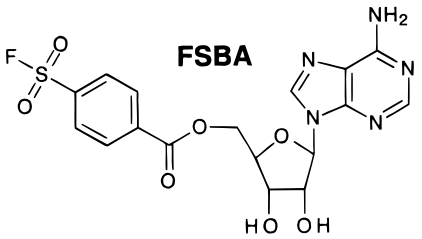

Labeling of specific amino acids with an affinity label is not always an indication that these residues are required for binding or catalysis. Numerous examples show the importance of confirming the proposed role of amino acids through the use of a complementary methodology such as site-directed mutagenesis (*13*, *14*) or structure determination (*15*, *16*).

This paper describes the use of FSBA (*17*) as an ATP affinity label for *E. coli* AIR synthetase (*1*). Enzyme inactivation is shown to occur stoichiometrically with specific labeling of a single amino acid residue. The peptide containing this residue has been isolated and sequenced, identifying the modified residue as Lys27. Site-directed mutagenesis of this residue has provided further insight into the ATP binding site. A comparison between the *E. coli* AIR synthetase and the trifunctional chicken liver protein containing AIR synthetase using the same approach is described (*18*, *19*). This work is complementary to the recent structural determination of AIR synthetase in the absence of any organic ligands (*4*).

MATERIALS AND METHODS

Materials. Sephadex G-25 and G-50 were obtained from Pharmacia. *E. coli* lactate dehydrogenase (LDH, 860 units/mg), pyruvate kinase (PK, 470 units/mg), phosphoenolpyruvate (PEP), reduced β-nicotinamide adenine dinucleotide phosphate (NADH), gelatin, bovine serum albumin (fraction V, BSA), FSBA, and adenosine 5′-triphosphate (ATP) were purchased from Sigma Chemical Co. [γ-^{32}P]-ATP (6000 Ci/mmol) and [8-^{14}C]FSBA (55 mCi/mmol) were obtained from New England Nuclear. HPLC reverse-phase C18 columns (4.6 × 250 mm) used in purification of peptides were purchased from Vydac. Dithiothreitol (DTT) was purchased from Amresco (Solon, OH). S¢intA scintillation fluid was purchased from Packard. The synthesis of FGAM, as a 40:60 α/β mixture, was accomplished as described by Mueller (*20*). FGAM is a mixture of anomers, and concentrations are given for the β anomer. Taq polymerase was from Perkin-Elmer. T4 DNA ligase was purchased from BRL. All restriction enzymes as well as *Hin*dIII- and *Bst*EII-digested λ DNA molecular weight standards were purchased from New England Biolabs. Oligonucleotides for sequencing and site-directed mutagenesis were obtained from the MIT Biopolymers Lab. Mermaid, glass beads for purification of oligomers <200 bp, was purchased from American Bioanalytical. USBioclean, glass beads for purification of DNA >200 bp, was purchased from the United States Biochemical Corp. *E. coli* strain TX635 (F′ *lac*Z$^+$ *c*I857), which contains an episome-borne temperature-sensitive λ repressor (*21*), pJS119, a plasmid containing purM under the control of a λp_L promoter (*22*), and TX393 [*ara* Δ (*lac*) *pur*M *srl*C300::Tn10 *rec*A56] (*23*) were gifts from Dr. John Smith and Louise Thomas of Seattle Biomedical Research Institute, Seattle, WA.

General Methods. Sodium dodecyl sulfate−polyacrylamide gel electrophoresis (SDS−PAGE) samples were prepared and run as described by Laemmli (*24*) and developed using the alternate fix and staining technique described by Cooper (*25*). Protein assays were accomplished using the method of Lowry et al. (*26*) with BSA [ϵ_{279} = 0.667 mL mg^{-1} cm^{-1} (*27*)] as a standard. Protein sequencing was effected using an Applied Biosystems Model 477 protein sequencer with an on-line Model 120 PTH amino acid analyzer by the MIT Biopolymers Lab. Small-scale (~10 μg) plasmid preparations were accomplished using the Magic Miniprep system from Promega, and larger scale plasmid isolation was effected using the Maxiprep kit from Qiagen. The DNA of all site-directed mutants prepared in this work was sequenced using a kit from BRL Life Sciences which employs Sequenase and the dideoxy chain termination method (*28*). Mass spectral analysis was performed on an Applied Biosystems Biopolymer Mass Analyzer, BIO-ION 20. Radioactivity was quantitated using a Packard 1500 Tri-Carb Scintillation Counter. Purification of short (<200 bp) oligomers was effected on acrylamide gels in Tris−borate EDTA buffer (TBE), whereas larger DNA samples were purified using 1% agarose and Tris−acetate EDTA (TAE) buffer (*29*). Competent cells were made using the method of Hanahan (*29*). Activity assays for AIR synthetase, both Bratton−Marshall and spectrophotometric, were as previously described (*19*). One unit of activity is defined as the amount of enzyme needed to form 1 μmol of product in 1 min at 37 °C.

Kinetics of AIR Synthetase Inactivation by FSBA. Inactivation reactions were carried out at 15 °C and contained 50 mM HEPES (pH 7.7), 3 mM $MgCl_2$, 400 mM KCl, 0.14 mM β-FGAM ($\alpha\beta$ mix), 2.7% (v/v) DMSO, 2.7% (v/v) ethanol, and 0.3 unit of AIR synthetase in a final volume of 100 μL. FSBA concentrations ranged from 0 to 440 μM. Enzyme concentrations were too high to assay from this mixture directly, and so after initiating the reaction with enzyme, 10 μL aliquots were removed at various times and diluted 1:10 into 90 μL of buffer containing 50 mM HEPES (pH 7.7), 3 mM $MgCl_2$, and 400 mM KCl. From this diluted sample, exactly 30 s after removing the enzyme from the inactivation mixture, a 10 μL aliquot was used to initiate an activity assay (Bratton−Marshall procedure) (*19*). Inactivation studies were also carried out (separately) with either the omission or the addition of FGAM or ADP, respectively, to the inactivation mixture.

Analysis of the inactivation data was performed using eq 2 (*30*), where E is enzyme activity at time t and E_0 represents the activity at time zero. Data from multiple inactivation experiments were fit to eq 3, to determine K_i, the dissociation constant for binding of FSBA to AIR synthetase, and k_2, the rate constant for inactivation.

$$\log\left(\frac{E}{E_0}\right) = -\left(\frac{k_{obs}}{2.303}\right) \times t \qquad (2)$$

$$\frac{1}{k_{obs}} = \left(\frac{K_i}{k_2}\right)\left(\frac{1}{I}\right) + \frac{1}{k_2} \qquad (3)$$

Stability of FSBA. Samples of FSBA (2.4 mM) were prepared in D_2O and contained 10% (v/v) DMSO-d_6, 9 mM

EDTA, and 90 mM potassium phosphate (pH 6, 7, or 8) in a final volume of 600 μL and kept at 4 °C. NMR spectra were taken periodically over a 3 week period. Control experiments were carried out in which adenosine (2.5 mM) replaced FSBA. The pD values of the solutions were redetermined at the end of each experiment.

Stoichiometry of Inactivation by FSBA. Inactivation mixtures contained in a final volume of 180 μL the following: 50 mM HEPES (pH 7.7), 3 mM $MgCl_2$, 400 mM KCl, 0.29 mM β-FGAM, 1.5 mg (specific activity 3.3 units/mg) of AIR synthetase, and either 0 or 0.23 mM FSBA. After a 3 h incubation at 15 °C, samples were loaded onto a Sephadex G-50 column (0.75 × 20 cm) equilibrated in 50 mM potassium phosphate (pH 6.5). Fractions of 0.5 mL were collected, and the fraction containing the protein was assayed for activity (Bratton−Marshall) and the protein concentration was determined (Lowry). Difference spectra were recorded using the control sample (0 mM FSBA) as a reference, with care being taken to ensure that the protein concentrations were equal in sample and reference cuvettes. The ϵ_{259} for FSBA used was 15 800 M^{-1} cm^{-1} (*17*).

Alternately, [^{14}C]FSBA was employed to measure the stoichiometry of inactivation. A typical reaction mixture contained 440 μM β-FGAM, 440 μM [8-^{14}C]FSBA (specific activity 1.1 × 10^6 cpm/μmol), and 2.1 mg of AIR synthetase in a final volume of 200 μL. Aliquots of 20 μL were removed at 0, 5, 10, 25, 45, 90, 120, and 180 min and placed on separate Sephadex G-50 columns (0.75 × 17 cm) equilibrated with 100 mM sodium phosphate (pH 7.0). Fractions of 0.5 mL were collected, and the fractions containing the protein were pooled and assayed for activity. The amount of radiolabel was quantitated by scintillation counting.

Stability of the E. coli AIR Synthetase−FSBA Adduct. A reaction mixture contained in a final volume of 400 μL 50 mM HEPES (pH 7.7), 3 mM $MgCl_2$, 400 mM KCl, 570 μM [^{14}C]FSBA (specific activity 3.1 × 10^6 cpm/μmol), 550 μM β-FGAM, 4.3 mg of AIR synthetase (specific activity 3.3 units/mg), and 15% (v/v) DMSO. The mixture was preincubated at 25 °C and the reaction initiated by addition of enzyme. Aliquots of 10 μL were removed at 2, 21, 60, and 180 min and loaded onto separate columns of Sephadex G-50 (0.75 × 10 cm) at 4 °C equilibrated in 100 mM sodium phosphate (pH 6.5). Fractions of ∼300 μL were collected. The fractions containing protein were pooled and assayed for activity. At 4.5 h, the time calculated to give 99% inactivation, four 85 μL aliquots of this inactivation mixture were loaded onto separate Sephadex G-50 columns (0.75 × 20 cm) at 4 °C, equilibrated in 0.1% (v/v) trifluoroacetic acid (TFA), 50 mM triethylammonium acetate (TEA·OAc) (pH 6.0), 100 mM sodium phosphate (pH 7.0), and 50 mM HEPES (pH 7.5), respectively. Fractions of 0.5 mL were collected, and the fractions containing protein were pooled. The samples containing protein−FSBA adducts in TEA·OAc, sodium phosphate, and HEPES buffers were incubated at 25 °C, while the sample in TFA was incubated at 4 °C. At various times (every ∼12 h over 96 h), a 100 μL aliquot was removed from each sample, placed onto a Centricon containing a 10 000 molecular weight cutoff filter (Ultrafree MC), and spun at 2000*g* for 60 min. The radioactivity in the filtrate and that retained on the filter were quantitated by scintillation counting. Control experiments were performed to ensure the filters used above did not cause ^{14}C quenching.

Isolation of E. coli AIR Synthetase−FSBA-Labeled Peptide. All yields in this section refer to the overall yield, and are normalized to the amount of protein (110 nmol) in the original inactivation. A reaction mixture identical to that previously described but containing 675 μM [^{14}C]FSBA (specific activity 2.7 × 10^6 cpm/μmol), 550 μM β-FGAM, 5% (v/v) DMSO, 10% (v/v) ethanol, and 4.2 mg (110 nmol) of AIR synthetase was incubated at 30 °C in a final volume of 220 μL. The reaction, initiated by addition of enzyme, was allowed to proceed for 3.5 h. The entire mixture was then loaded onto a Sephadex G-50 column (0.75 × 20 cm) in 50 mM HEPES (pH 7.5) at 4 °C and eluted with the same buffer. Fractions (300 μL) were collected, and those containing protein were pooled. Solid guanidine hydrochloride and stock solutions of HEPES, EDTA, and DTT were added to this mixture, and the solution was adjusted to pH 7.5 using 1 M NaOH. The mixture contained, in a final volume of 1.2 mL, 5.4 M guanidine hydrochloride, 100 mM HEPES (pH 7.5), 10 mM EDTA, ∼90 μM protein, and 1 mM DTT. Reduction of the disulfide bonds was accomplished by incubating this reaction mixture at 25 °C for 30 min. Iodoacetic acid was then added to give a final concentration of 5 mM. The reaction vessel was wrapped in foil and incubated at 25 °C for 3 h, after which the solution was loaded onto a Sephadex G-50 column (1.5 × 18 cm) at 4 °C in 100 mM sodium phosphate (pH 7.0) and eluted with the same buffer. Fractions (0.5 mL) were collected and analyzed for A_{280} and radioactivity by scintillation counting. Fractions containing protein were pooled (5 mL), and the protein concentration was determined (*26*). The recovery of protein through the inactivation and carboxymethylation steps was 52% (58 nmol). Trypsin (2.2 μL of 10 mg/mL, 580 pmol) was added to this sample containing inactivated AIR synthetase. After 6 h at 37 °C, conditions determined by control experiments to give complete digestion, the reaction mixture was frozen in liquid N_2 and stored at −80 °C.

The proteolyzed [^{14}C]AIR synthetase was purified using a Vydac C18 analytical column (4.6 × 250 mm) equilibrated in 0.1% (v/v) TFA in water (solvent A), and eluted with an increasing 0.1% (v/v) TFA in acetonitrile gradient. [^{14}C]-Adduct (9 nmol) in 1 mL was injected onto the column which was eluted at 1 mL/min. One minute fractions were collected. A single radioactive peak eluted at 37% (v/v) acetonitrile using a linear gradient of 0−60% acetonitrile/0.1% TFA over 75 min (Figure 1). Fractions containing radioactivity from all five injections were pooled and concentrated in vacuo, but not to dryness, to a final volume of 980 μL. Radioactivity recovered through this step was 25% (30 nmol) of the initial adduct. The [^{14}C]adduct was then rechromatographed in a second solvent system using 20 mM sodium phosphate (pH 7.0) as solvent A and 70% CH_3CN in 20 mM sodium phosphate (pH 7.0) as solvent B. Each injection contained 15 nmol of adduct in 500 μL, and a single radioactive peak was isolated at 39 min using 30% B in an isocratic elution (Figure 1, inset). Fractions containing radioactivity were pooled and concentrated in vacuo to 350 μL (*not* to dryness). Quantitation revealed that the overall yield of radioactivity through this second isolation was 17% (19 nmol). This material was then desalted using the TFA system described above. Again, a single peak eluted at 38% acetonitrile/0.1%

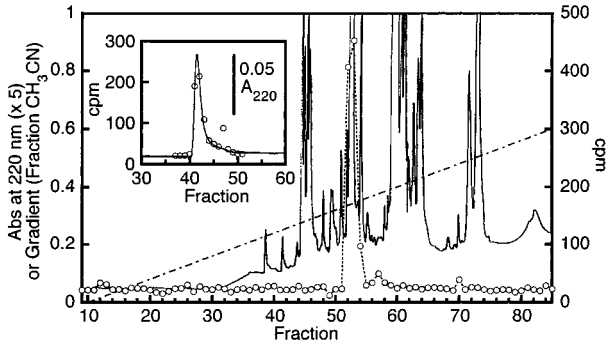

FIGURE 1: Isolation of a FSBA−AIR synthetase adduct using Vydac C18 reverse phase HPLC and aqueous TFA in an acetonitrile gradient. The A_{220} profile of the initial purification (solid line) with the elution gradient is indicated on the axis at the left (dash−dot line). The radioactive profile of fractions eluted from the column (○, dotted line) is given by the axis on the right. Inset: Reisolation of a FSBA−AIR synthetase adduct using Vydac C18 reverse phase HPLC and sodium phosphate in an acetonitrile gradient. Appropriate fractions from the purification shown in the main figure were rechromatographed using an isocratic gradient of 30% B (see text for buffer compositions) at a flow rate of 1 mL/min. Fractions were collected every 30 s, and an aliquot of each was quantitated by scintillation counting.

TFA, and fractions containing radioactivity were pooled and concentrated to 520 μL in vacuo (again, *not* to dryness). The adduct was isolated in a final yield of 14% (15 nmol). This sample was submitted for Edman degradation and mass spectral analysis.

Analysis of the Interaction of Chicken Liver AIR Synthetase (purDMN) with FSBA. Incubation mixtures contained 50 mM HEPES (pH 7.7), 20 mM $MgCl_2$, 200 mM KCl, 9% (v/v) DMSO, 0.1 mM β-FGAM, 1.3×10^{-2} unit of AIR synthetase (specific activity 0.45 unit/mg), and either 10 μM, 0.1 mM, or 1 mM FSBA in a final volume of 55 μL. A control reaction was identical to that described above except that FSBA was omitted. Incubations were carried out at 25 °C, and the reaction was initiated by addition of FSBA. Aliquots were removed at 0.5, 5, 15, 30, and 45 min, and AIR synthetase activity was determined using the Bratton−Marshall assay (*19*). Results were analyzed using eq 2 as above.

Preparation of Site-Directed Mutants of E. coli AIR Synthetase. Mutants were prepared by the method of Taylor et al. (*31*), using a kit from Amersham (version 2). M13 ds DNA was isolated using Magic Minipreps. DNA containing the *pur*MN gene was isolated as a 2 kb fragment from an *Eco*RI/*Bam*HI digest of pJS119, and purified on a 1% agarose gel before use in subsequent ligations. M13mp18 DNA was likewise digested with *Eco*RI/*Bam*HI and purified on a 1% agarose gel. Ligations were run for 14 h at 25 °C and contained 60 ng of purMN fragment and 25 μg of M13-derived DNA with 1 unit of T4 DNA ligase (BRL) in 10 μL. Transformation of *E. coli* TG1 bacteria (*29*) with 5 μL of ligation mixture and growth on media containing isopropyl β-D-thiogalactopyranoside (IPTG) and 5-bromo-4-chloro-3-indolyl β-galactoside yielded 10 colorless plaques.

Single-stranded M13mp18 DNA containing *pur*MN was isolated by standard procedures (*29*). Mutagenesis was accomplished with this ss DNA and the primers L, Q, and R (Table 1) and the procedure outlined in the Amersham kit.

The 2 kb DNA fragment of the replicative form of each mutant was isolated, digested with *Eco*RI and *Bam*HI, and purified on 1% agarose. This DNA was ligated with the 3 kb gel-purified fragment from *Eco*RI/*Bam*HI-digested pJS119, using a insert:vector ratio of (3−5):1 (~600 ng of vector DNA). Ligation mixtures were used to transform either *E. coli* strain TX635 or TX393. Transformants were selected on LB media with 50 μg/mL ampicillin, and a small number of the resulting >100 colonies were analyzed using restriction analysis and subsequent DNA sequencing of the entire *pur*M gene. All transformants sequenced contained the expected base changes.

Table 1: Primers Used in Mutagenesis[a]

primer	sequence (5′ → 3′)
L	GCC TAG GAT TCT TCC AAC CAG
Q	GCC TTG GAT TCT TCC AAC CAG
R	GCC TCT GAT TCT TCC AAC CAG

[a] Underlined regions identify mutated codons.

Defining Growth Conditions for TX635/pJS119 K27X Mutants. To optimize the growth conditions for pJS119 [containing wild type (wt) and mutants] in *E. coli* strain TX635, the bacteria were grown in LB media at 30 °C. Aliquots were removed just before heat induction to 42 °C and then at 1, 2, 3, and 4 h after induction. Each sample was spun for 1 min in an Epifuge at 4 °C, the supernatant was removed, and the pellet was quick-frozen in liquid nitrogen. Each sample was then resuspended in 10 mM Tris-HCl (pH 7.5) such that an aliquot would produce an A_{600} of 0.075 OD. A 40 μL aliquot of this resuspended sample was added to 10 μL of 5× Laemmli buffer (*24*) and placed in a boiling water bath for 5 min. These samples were then loaded onto a 10% acrylamide gel and subjected to SDS−PAGE.

The doubling time of each overproducing strain was 0.9 h, identical to the pJS119 wt strain. Bacteria were induced in late log phase (~0.6−0.8 OD_{600}) by adding an equal volume of media at 54 °C with rapid stirring. The cultures were transferred to a 42 °C incubator and allowed to grow for another 4 h.

Growth of K27X Mutants of AIR Synthetase from TX393/pJS119. Studies in the previous section revealed that mutant AIR synthetases were expressed constitutively. TX393 strains were grown at 30 °C in LB media and were harvested 3 h after their transition into stationary phase. Cells were collected by centrifugation (10 min, 2700*g* at 4 °C), and stored at −80 °C. Cell paste yields from a 1 L culture were 1.5−2.8 g.

Isolation and Characterization of K27X Mutants. Isolation of wt and mutant *E. coli* AIR synthetases was as described by Schrimsher et al. (*1*), except that the final size exclusion column was omitted. The apparent $K_{m,ATP}$ for each Lys27 mutant AIR synthetase was determined. A typical reaction mixture contained the following in a final volume of 300 μL: 50 mM HEPES (pH 7.7), 3 mM $MgCl_2$, 970 mM KCl, 230 μM β-FGAM, 2 mM PEP, 0.2 mM NADH, 10 unit of PK, 10 units of LDH, AIR synthetase, and varied amounts of ADP ($0.2-5 \times K_m$). Data were fit to the Michaelis−Menten equation using the programs of Cleland (*32*).

RESULTS

Kinetics of Inactivation of AIR Synthetase by FSBA. FSBA is an ATP analogue that has been successfully used to covalently modify the ATP binding site of a number of

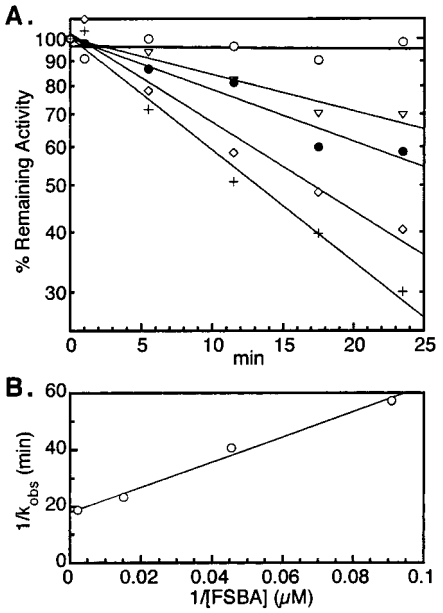

FIGURE 2: (A) Time-dependent inactivation of AIR synthetase by FSBA. AIR synthetase was incubated with (○) 0, (▽) 11 μM, (●) 22 μM, (◇) 66 μM, and (+) 440 μM FSBA. (B) Determination of the inactivation constants using eq 3 and a plot of $1/k_{obs}$ vs 1/[FSBA].

proteins (*5*, *6*). In an effort to label the active site of AIR synthetase, various concentrations of FSBA were incubated with the enzyme and saturating amounts of FGAM, and at various times aliquots were removed and assayed for enzyme activity. The results shown in Figure 2A reveal time-dependent inactivation. The model describing this process is given in eq 4, where E is enzyme, I is the inhibitor, K_i is the thermodynamic dissociation constant, and k_2 is the rate constant for inactivation.

$$E + I \overset{K_i}{\rightleftharpoons} E{\cdot}I \xrightarrow{k_2} E{-}I^* \qquad (4)$$

A replot of the data obtained from Figure 2A using eq 3 (Materials and Methods) gives a straight line (Figure 2B) from which the kinetic constants, $K_i = 25$ μM and $k_2 = 5.6 \times 10^{-2}$ min^{-1}, were determined (*33*). This K_i for FSBA is similar to the previously reported apparent K_m for ATP of 65 μM (*1*). The rate of inactivation is 1/40th the rate constant for turnover with the natural substrate.

A repetition of these experiments in the absence of FGAM gave a 2-fold reduction in the rate of inactivation, and in the presence of ADP (100 μM) gave complete protection against inactivation (data not shown). ADP, a competitive inhibitor with respect to ATP (*1*), was used in these protection experiments instead of ATP to avoid turnover. The effects of FGAM and ADP both suggest that inactivation occurs through a specific interaction between the inhibitor and AIR synthetase.

Stoichiometry of Inactivation by FSBA. Control experiments revealed that AIR synthetase (at concentrations >0.8 mg/mL) is stable over a 90 min incubation at 30 °C in the absence of inhibitor. Thus, these conditions were chosen to examine the stoichiometry of its inactivation by FSBA. [^{14}C]-FSBA was used to follow the stoichiometry of adduct/enzyme formation during the course of an inactivation. The results of a typical reaction are shown in Figure 3. These results indicate that despite the slow rate of inactivation, the

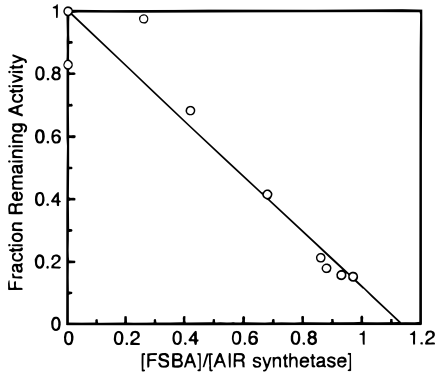

FIGURE 3: Stoichiometry of FSBA−AIR synthetase adduct measured using [^{14}C]FSBA. The protein concentration (Lowry) and the radioactivity (scintillation counting) were determined for each sample. Extrapolation to total inactivation suggests that 1.1 adducts per AIR synthetase completely inactivate the enzyme.

Table 2: Stability of the [^{14}C]FSBA−AIR Synthetase Adduct[a]

time (h)	TFA (pH 2)	TEA·OAc (pH 6)	NaP_i (pH 7)	HEPES (pH 7.5)
0	0.99	0.99	0.99	1.0
24	0.98	0.98	nd	0.88
48	0.98	0.98	0.83	0.97
84	0.96	0.97	0.92	0.92

[a] Data presented as fraction of label bound.

labeling is stoichiometric with 1.1 ± 0.2 FSBA per active site, and suggest that there is a specific interaction between the inhibitor and the enzyme. However, these experiments do not distinguish between a covalently bound and a tightly bound inhibitor.

Stability of FSBA. The stability of FSBA was studied, under a variety of pH conditions, to ensure that the ester linkage would be stable to the conditions required for peptide purification. The hydrolysis of FSBA to adenosine was monitored using NMR spectroscopy, by the appearance of its H8 and H2 protons (δ 8.17 and 8.07, respectively). Integration of the signal associated with the H2 proton at various times allows a kinetic analysis of the hydrolysis process. From this analysis, a half-life for FSBA at pH 7.0 can be extrapolated to be ~2 months, and at pH 8, 13 days. No measurable decomposition of inhibitor at pH 5.5 was found after 450 h. These results agree with those previously reported by Esch and Allison (*34*) using adenosine deaminase to monitor adenosine formation. They found the half-life of FSBA at 23 °C (pH 8) to be 3.6 days.

Stability of the E. coli AIR Synthetase−FSBA Adduct. The stability of the linkage of the AIR synthetase−FSBA adduct was also determined, to define the conditions required to purify the modified FSBA-containing peptide(s). These experiments used Centricons and size exclusion filters to separate enzyme-bound [^{14}C]FSBA adduct from ^{14}C-labeled small molecules. Control experiments revealed that the filters used in this study caused no quenching of ^{14}C-labeled material and that all of the radioactivity could be recovered.

Results from the stability experiments are summarized in Table 2. From these data it is clear that the AIR synthetase·FSBA adduct is stable in all buffers tested for at least 84 h. The stability of the adduct suggests that either a Lys or a Tyr is modified by FSBA.

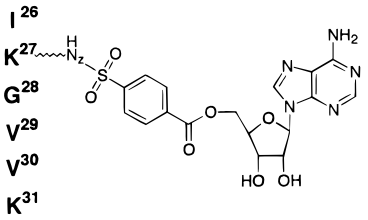

FIGURE 4: Proposed structure of the FSBA-modified tryptic peptide from AIR synthetase.

Isolation of the E. coli AIR Synthetase−FSBA-Labeled Peptide. FSBA-inactivated AIR synthetase (110 nmol) was subjected to carboxymethylation and trypsin digestion, and the peptides were isolated using a Vydac C18 reverse phase column with TFA/CH_3CN elution as shown in Figure 1. The fractions containing the radiolabel were pooled, lyophilized, and reanalyzed using the sodium phosphate (pH 7)/acetonitrile elution shown in Figure 1 (inset). Lyophilization of the peptide to dryness at any stage during the purification resulted in extremely poor recoveries. The peptide isolated is the major adduct of FSBA inactivation and was recovered in 14% overall yield.

The peptide was sequenced using the automated Edman degradation method to give I-X-G-V-V-K. This sequence is consistent with the expected AIR synthetase tryptic fragment:

```
...G   R ^ I   K ^ G   V   V   K ^ K ^ T...
  24  25  26  27  28  29  30  31  32  33
```

where the circumflex indicates a position predicted to be cleaved by trypsin and the sequence of interest is underlined. It is interesting to note that if the Lys at position 27 were alkylated, trypsin would no longer be expected to cleave after that residue. Thus, the sequence is consistent with the adduct stability data and the fact that trypsin was used to digest the protein. In the second Edman degradation cycle, one major and one minor PTH-amino acid peak eluted between Tyr- and Pro-PTH derivatives. N^{ϵ}-(4-Carboxybenzenesulfonyl)-lysine has previously been shown to elute with a similar retention time (*35*). The major peak is thus likely to be the PTH derivative of the FSBA-modified Lys27.

Characterization of the FSBA−AIR Synthetase Adduct. In an attempt to define the structure of the FSBA adduct on the peptide, plasma desorption mass spectrometry was performed. The resulting parent peak of 1077.3 amu (data not shown) is consistent with the expected structure (Figure 4), which has a calculated MH^+ of 1077.25 amu.

Incubation of Chicken Liver AIR Synthetase with FSBA. After successfully determining the site of interaction of FSBA with *E. coli* AIR synthetase, we were curious to find if FSBA also modified the enzyme from chicken liver in the same manner. AIR synthetase from this source is a trifunctional protein containing an N-terminal glycinamide ribonucleotide (GAR) synthetase and a C-terminal GAR-transformylase in addition to AIR synthetase (*18, 19*). Sequence comparisons show that the chicken liver enzyme has 68% sequence similarity and 51% identity with the *E. coli* enzyme. The chicken liver enzyme was incubated in the presence of FGAM and FSBA (1 mM). No inactivation was detected after 45 min (data not shown).

Mutagenesis of E. coli AIR Synthetase (pJS119). With the site of interaction between FSBA and *E. coli* AIR synthetase determined, site-directed mutagenesis of Lys27 to Gln, Leu, or Arg was employed to substantiate the importance of this residue suggested by the labeling studies. Mutagenesis was accomplished using the method of Taylor et al. (*31*). Sequencing of the −84 through 173 bp region of the newly generated *pur*M genes indicated that each of the desired mutants had been successfully prepared. However, three cytosines were found to be absent from the −50 through −52 region in all mutant constructs. Despite this, the reading frames for translation remain intact, and the proteins are expressed at high levels. However, protein production is no longer heat-inducible as is observed with the wt construct.

Table 3: Kinetic Parameters for K27X AIR Synthetases

enzyme	$K_{m,ATP}$ (μM)	k_{cat} (s^{-1})	V/K (s^{-1} μM^{-1} × 10^2)
wt[a]	73 ± 14	2.3 ± 0.1	3.5 ± 0.8
K27Q	58 ± 4.5	3.0 ± 0.2	5.2 ± 0.75
K27L	46 ± 3.1	2.6 ± 0.1	5.7 ± 0.60
K27R	12 ± 1.1	2.5 ± 0.1	21.0 ± 2.9

[a] Redetermined in these studies.

Growth and Induction of pJS119 K27X Mutants. The doubling times for *E. coli* TX635/pJS119 mutants were indistinguishable from identical constructs expressing the wt enzyme when grown in LB media. The bacteria, containing mutant or wt AIR synthetase, doubled every 0.9 h. The optimum time to harvest the mutants was found to be 1−2 h after reaching the late log phase of growth; AIR synthetase levels slowly decrease after that time (data not shown). When enzyme was expressed in host strain TX393 (*pur*M^-), the growth of the strains producing mutant enzymes was also indistinguishable from the wt-expressing system, with doubling times of 1.3 h.

Isolation and Determination of $K_{m,ATP}$ for AIR Synthetase K27X Mutants. AIR synthetase mutants were purified by a procedure identical to that described for wt AIR synthetase (*1*). The crucial purification step uses a C8-linked ATP affinity column. The mutant enzymes are retained in the same way as the wt protein, suggesting similarities in their ATP binding sites. Mutant proteins were ∼80% pure, as judged by SDS−PAGE, while the wt protein was purified to homogeneity using the same procedure.

The kinetic parameters for the mutants were measured using substrate concentrations that are saturating for the wt enzyme (Table 3). A complete kinetic analysis of the mutants has not yet been carried out. The specific activities of the mutant enzymes were, in contrast to expectations, all slightly higher than that observed for the wt AIR synthetase. Even more surprising was that the $K_{m,ATP}$ for each mutant was lower than the $K_{m,ATP}$ (65 μM) previously determined for the wt protein (*1*). The K27R mutant has an apparent $K_{m,ATP}$ 5-fold lower than the wt enzyme. The identification of Lys27 in the ATP binding domain using FSBA suggested to us initially that it might play an important role in charge neutralization in phosphate binding. The mutagenesis results, however, suggest an alternative role for Lys in the ATP binding domain is required.

DISCUSSION

FSBA interacts with *E. coli* AIR synthetase as an active site affinity label, covalently modifying the enzyme specifically at Lys27. ADP protects AIR synthetase against

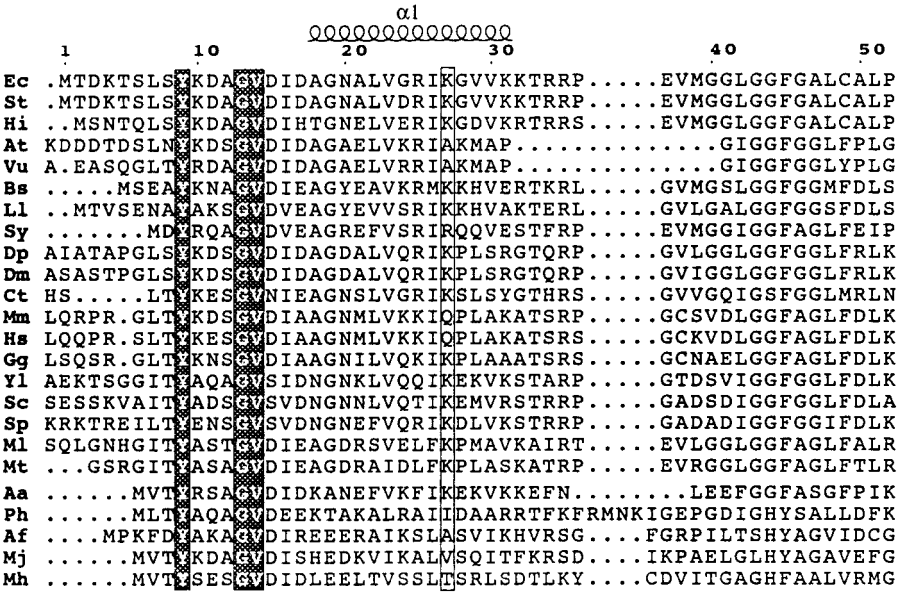

FIGURE 5: Alignment of AIR synthetases from various organisms. The alignment was calculated using the full sequence of each protein, and ClustalW (*36*). The coil at the top indicates the kinked helix (α1). Shaded residues are absolutely conserved. The position of Lys27 is boxed. Mesophile (top) and thermophile (bottom) sequences are separated because of differences in the Gly-rich loop region. The amino terminus of each protein is shown in the figure unless the number of the first amino acid in the figure is given in brackets. Key to abbreviations: bacteria and plants: Ec, *E. coli* (*23*); St, *S. typhimurium* (J. L. Zillies and D. M. Downs, unpublished observations); Hi, *H. influenzae* (*38*); At, *A. thaliana* [59] (*39*); Vu, *V. unguiculata* [61] (P. M. C. Smith, A. J. Mann, D. J. Hall, and C. A. Atkins, unpublished observations); Bs, *B. subtilis* (*40*); Ll, *L. lactis* (C. Coward, unpublished observations); Sy, *Synechocystis* (*41*); flies: Dp, *D. pseudoobscura* [435] (*42*); Dm, *D. melanogaster* [435] (*42*); Ct, *C. tentans* [437] (*43*); vertebrates: Mm, *M. musculus* [429] (*44*); Hs, *H. sapiens* [429] (*45*); Gg, *G. gallus* [429] (*45*); yeasts: Yl, *Y. lipolytica* [432] (C. A. Strick, L. C. James, K. E. Cole, and L. A. Elsenboss, unpublished observations); Sc, *S. cerevisiae* [443] (*46*); Sp, *S. pombe* [430] (*47*); mycobacteria: Ml, *M. leprae* [18] (D. R. Smith and K. Robison, unpublished observations); Mt, *M. tuberculosis* (*48*); thermophilic bacteria: Aa, *A. aeolicus* (*49*); Ph, *P. horikoshii* (*50*); thermophilic archaebacteria: Af, *A. fulgidus* (*51*); Mj, *M. janaschii*; Mh, *M. thermoautotrophicum* (*52*).

inhibition, while addition of FGAM to the inactivation mixture enhances the rate of inactivation. These studies suggest that FSBA acts on *E. coli* AIR synthetase at or near the ATP binding site.

The N-terminal sequences of 24 AIR synthetase genes from different organisms are aligned in Figure 5 using ClustalW (*36*). Although these enzymes share a large number of conserved residues, the Lys labeled by FSBA in the *E. coli* enzyme is not absolutely conserved. Human AIR synthetase has a Gln residue, and *Arabidopsis* AIR synthetase contains an Ala in this position. Furthermore, the chicken liver trifunctional enzyme, even though it contains a Lys at this position, is not inactivated by FSBA in the presence or absence of FGAM. The lack of complete conservation of Lys27 between organisms and the fact that the trifunctional protein is not inactivated foreshadow the results of the site-directed mutagenesis studies and provide insight about the function of this residue.

To further explore the function of Lys27 in *E. coli* AIR synthetase, it was mutated to Gln, Leu, and Arg. The apparent $K_{m,ATP}$ for each mutant was determined at 230 μM FGAM. Observation of $K_{m,ATP}$ values for the Leu and Gln mutants that are almost identical to that for the wt enzyme establishes that Lys27 clearly is not involved in charge neutralization of the phosphates of ATP. All of the mutant residues have hydrophobic side chains that these results suggest are important for ATP binding. This contribution may be direct or conformational. Even more striking is that the turnover number for the Gln mutant is 30% greater than that for the wt protein. The basis for the improved efficiency of mutant AIR synthetase over wt is at present unclear.

We have recently determined the crystal structure of sulfate-liganded *E. coli* AIR synthetase modified with an N-terminal hexa-His tag at 2.5 Å resolution (*4*). The structure reveals a dimer held together by extensive intersubunit interactions, in agreement with solution studies on this protein (*1*). The interfaces between the subunits create two large clefts, each of which is lined with many conserved residues (Figure 6). A sulfate ion is bound at the wider end of each cleft, and a flexible Gly-rich hairpin loop is 25 Å away at the other end of each cleft. A kinked helix extends in an arch over the cleft, presumed to be the active site. This helix separates the Gly-rich loop from a globular central core composed of domains from each subunit. The kinked helix (residues 17−31) is visible along its entire length in only one of the subunits. In the second subunit, residues 5 through 20 are not detectable. Lys27 is located at the kink in the helix (Figure 6).

The bound sulfate could be indicative of a phosphate binding site. However, it is unclear whether such a site would be associated with FGAM binding, ATP binding, or both. The FSBA inactivation studies provide important information allowing formulation of a model for substrate binding within the active site. FSBA acylates Lys27 in the kinked helix (Figure 6). These results have been interpreted to indicate that ATP binds near the Gly-rich hairpin, 20−30 Å away from the sulfate binding site. If our interpretation of the FSBA binding studies is correct, then the sulfate is probably indicative of the FGAM phosphate binding site. Sequence conservation, sulfate binding, and FSBA labeling together indicate that the cleft defines the active site of AIR synthetase. The FSBA studies have been particularly critical

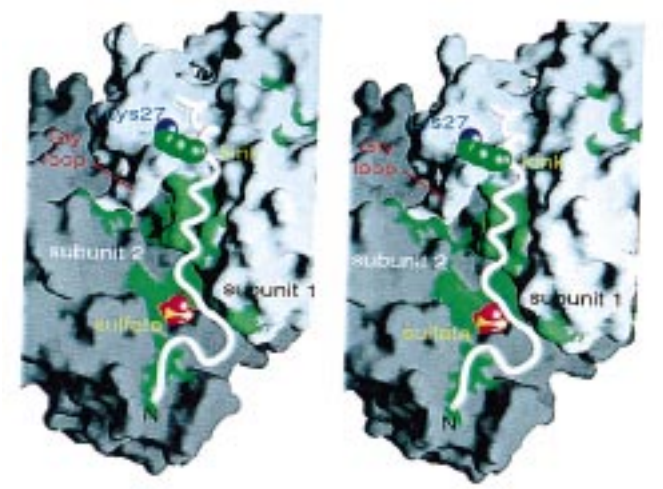

FIGURE 6: Stereoview of the putative active site cleft in *E. coli* AIR synthetase and the position of the sulfate relative to Lys27. A molecular surface is shown for the AIR synthetase dimer at the subunit interface, which defines the active site cleft. Green surfaces correspond to solvent-exposed, strictly conserved residues. Important structural features discussed in the text are labeled. The white ribbon is the kinked helix α1 (residues 5−34) from the lighter colored subunit 1. Sulfate and Lys27, which is located at the kink in the helix, are presented in CPK space-filling models with traditional colors.

as thus far we have been unable to crystallize either ATP or an FGAM analogue with AIR synthetase.

Lys residues are typical components of ATP binding sites, where they frequently interact electrostatically with the phosphate moieties. Several observations indicate that Lys27 in *E. coli* AIR synthetase may not perform this function and that it is located in a conformationally dynamic region of the enzyme. The crystal structure reveals that the side chain of Lys27 including its amino group points away from the putative active site cleft. This conformation leaves only the β- and γ-methylenes of Lys adjacent to the putative ATP binding pocket (Figure 6). Our mutagenesis studies indicate that the methylene linker and not the amino group of Lys plays a key role in defining the ATP binding domain.

The unliganded structure and the positioning of Lys27 are probably not indicative of the active protein conformation. As noted above, Lys27 is located on a dynamic kinked helix adjacent to a glycine-rich flexible loop (Figure 6). The flexibility of the helix is apparent by the differences in the N-terminus of the two subunits of AIR synthetase (*4*). In addition, the flexibility of the glycine-rich loop is indicated by this loop's higher than average *B* factors. Finally, efforts to soak ATP into apo AIR synthetase crystals resulted in their cracking. Thus, the structure of apo AIR synthetase is probably not indicative of the conformation of Lys27 with the FSBA bound. The efficiency of FSBA modification, its potentiation by FGAM, and its inhibition by ADP support labeling of the ATP binding domain as well as its conformational flexibility. The distance between Lys27 and the sulfate (Figure 6) suggests that an extended or partially extended nucleotide and FGAM can fit into the putative active site cleft. Definition of the detailed binding of ATP and the role of Lys27 in the active site will require a structure determination in the presence of nucleotides.

Subtle differences in conformation may also account for the observation that the trifunctional AIR synthetase is not inactivated by FSBA. This result was unexpected as the proteins are homologous and both contain Lys27. A major difference between the mono- and trifunctional synthetases, however, is that the trifunctional protein is tethered to GAR synthetase at its N-terminus. This fusion could affect the conformation of the flexible kinked helix and its short extension (16 residues to the N-terminus). Thus, despite the fact that Lys27 is present in the trifunctional protein, the additional protein domain attached to the N terminus of the trifunctional protein could affect lid movement over the active site cleft in a fashion different from the monofunctional AIR synthetase.

There is substantial literature (*11*, *37*) in which FSBA and other putative ATP analogues have provided information about the region surrounding the ATP binding site of different proteins. The tight binding of FSBA to *E. coli* AIR synthetase favors the hypothesis that FSBA has labeled a residue in the region in which ATP binds. Further biochemical studies in conjunction with structural information in the presence of nucleotides are required for further definition of the role of residue 27 in ATP binding.

REFERENCES

1. Schrimsher, J. L., Schendel, F. J., Stubbe, J., and Smith, J. M. (1986) *Biochemistry 25*, 4366−4371.
2. Schendel, F. J., Mueller, E., Stubbe, J., Shiau, A., and Smith, J. M. (1989) *Biochemistry 28*, 2459−2471.
3. Hardie, D. G., and Coggins, J. R. (1986) in *Multidomain Proteins: Structure and Evolution* (Hardie, D. G., and Coggins, J. R., Eds.) pp 1−12, Elsevier, New York.
4. Li, C., Kappock, T. J., Stubbe, J., Weaver, T. M., and Ealick, S. E. (1999) *Structure* (in press).
5. Colman, R. F. (1983) *Annu. Rev. Biochem. 52*, 67−91.
6. Colman, R. F. (1989) in *Protein Function, A Practical Approach* (Creighton, T. E., Ed.) pp 77−99, IRL Press, Oxford.
7. Pinkofsky, H. B., Ginsburg, A., Reardon, I., and Heinrikson, R. L. (1984) *J. Biol. Chem. 259*, 9616−9622.
8. Bitar, K. G. (1982) *Biochem. Biophys. Res. Commun. 109*, 30−35.
9. Poulos, T. L., and Price, P. A. (1974) *J. Biol. Chem. 249*, 1453−1457.
10. Krieger, T. J., and Miziorko, H. M. (1986) *Biochemistry 25*, 3496−3501.
11. Pandey, V. N., and Modak, M. J. (1988) *J. Biol. Chem. 263*, 6068−6073.
12. Harlow, K. W., and Switzer, R. L. (1990) *J. Biol. Chem. 265*, 5487−5493.
13. Parakh, C. R., and Villafranca, J. J. (1990) *Abstr. Pap.—Am. Chem. Soc. 199*, BIOL-111.
14. Freitag, N. E., and McEntee, K. (1991) *J. Biol. Chem. 266*, 7058−7066.
15. Vollmer, S. H., and Colman, R. F. (1990) *Biochemistry 29*, 2495−2501.
16. Kohlstaedt, L. A., Wang, J., Friedman, J. M., Rice, P. A., and Steitz, T. A. (1992) *Science 256*, 1783−1790.
17. Pal, P. K., Wechter, W. J., and Colman, R. F. (1975) *J. Biol. Chem. 250*, 8140−8147.
18. Daubner, S. C., Schrimsher, J. L., Schendel, F. J., Young, M., Henikoff, S., Patterson, D., Stubbe, J., and Benkovic, S. J. (1985) *Biochemistry 24*, 7059−7062.
19. Schrimsher, J. L., Schendel, F. J., and Stubbe, J. (1986) *Biochemistry 25*, 4356−4365.
20. Mueller, E. J. (1994) Ph.D. Thesis, Massachusetts Institute of Technology.
21. Mieschendahl, M., and Müller-Hill, B. (1985) *J. Bacteriol. 164*, 1366−1369.
22. Inglese, J., Johnson, D. L., Shiau, A., Smith, J. M., and Benkovic, S. J. (1990) *Biochemistry 29*, 1436−1443.

23. Smith, J. M., and Daum, H. A., III (1986) *J. Biol. Chem. 261*, 10632−10636.
24. Laemmli, U. K. (1970) *Nature 227*, 680−685.
25. Cooper, T. (1977) *The Tools of Biochemistry*, John Wiley & Sons, New York.
26. Lowry, O. H., Rosenbrough, N. J., Farr, A. L., and Randall, R. J. (1951) *J. Biol. Chem. 193*, 265−275.
27. Schachman, H. D., and Edelstein, S. J. (1966) *Biochemistry 5*, 2681−2675.
28. Sanger, F., Nicklen, S., and Coulson, A. R. (1977) *Proc. Natl. Acad. Sci. U.S.A. 74*, 5463−5467.
29. Sambrook, J., Fritsch, G. F., and Maniatis, T. (1989) *Molecular Cloning: A Laboratory Guide*, Cold Spring Harbor Laboratory Press, Cold Spring Harbor, NY.
30. Foster, W. B., Griffith, M. J., and Kingdon, H. S. (1981) *J. Biol. Chem. 256*, 882−886.
31. Taylor, J. W., Ott, J., and Eckstein, F. (1985) *Nucleic Acids Res. 13*, 8765−8785.
32. Cleland, W. W. (1979) *Methods Enzymol. 63*, 103−138.
33. Main, A. R. (1973) in *Essays in Toxicology* (Hays, J. W., Eds) pp 59−105, Academic Press, New York.
34. Esch, F. S., and Allison, W. S. (1978) *J. Biol. Chem. 253*, 6100−6106.
35. Saradambal, K. V., Bednar, R. A., and Colman, R. F. (1981) *J. Biol. Chem. 256*, 11866−11872.
36. Thompson, J. D., Higgins, D. G., and Gibson, T. J. (1994) *Nucleic Acids Res. 22*, 4673−4680.
37. Beese, L. S., Friedman, J. M., and Steitz, T. A. (1993) *Biochemistry 32*, 14095−14101.
38. Fleischmann, R. D., Adams, M. D., White, O., Clayton, R. A., Kirkness, E. F., Kerlavage, A. R., Bult, C. J., Tomb, J. F., Dougherty, B. A., Merrick, J. M., McKenney, K., Sutton, G., Fitzhugh, W., Fields, C., Gocayne, J. D., Scott, J., Shirley, R., Liu, L. I., Glodek, A., Kelley, J. M., Weidman, J. F., Phillips, C. A., Spriggs, T., Hedblom, E., Cotton, M. D., Utterback, T. R., Hanna, M. C., Nguyen, D. T., Saudek, D. M., Brandon, R. C., Fine, L. D., Fritchman, J. L., Fuhrmann, J. L., Geoghagen, N. S. M., Gnehm, C. L., McDonald, L. A., Small, K. V., Fraser, C. M., Smith, H. O., and Venter, J. C. (1995) *Science 269*, 496−512.
39. Senecoff, J. F., and Meagher, R. B. (1993) *Plant Physiol. 102*, 387−399.
40. Ebbole, D. J., and Zalkin, H. (1987) *J. Biol. Chem. 262*, 8274−8287.
41. Kaneko, T., Tanaka, A., Sato, S., Kotani, H., Sazuka, T., Miyajima, N., Sugiura, M., and Tabata, S. (1995) *DNA Res. 2*, 153−166.
42. Henikoff, S., and Eghtedarzadeh, M. K. (1987) *Genetics 117*, 711−725.
43. Clark, D. V., and Henikoff, S. (1992) *J. Mol. Evol. 35*, 51−59.
44. Kan, J. L., Jannatipour, M., Taylor, S. M., and Moran, R. G. (1993) *Gene 137*, 195−202.
45. Aimi, J., Qiu, H., Williams, J., Zalkin, H., and Dixon, J. E. (1990) *Nucleic Acids Res. 18*, 6665−6672.
46. Henikoff, S. (1986) *J. Mol. Biol. 190*, 519−528.
47. McKenzie, R., Schuchert, P., and Kilbey, B. (1987) *Curr. Genet. 12*, 591−597.
48. Cole, S. T., Brosch, R., Parkhill, J., Garnier, T., Churcher, C., Harris, D., Gordon, S. V., Eiglmeier, K., Gas, S., Barry, C. E., III, Tekaia, F., Badcock, K., Basham, D., Brown, D., Chillingworth, T., Connor, R., Davies, R., Devlin, K., Feltwell, T., Gentles, S., Hamlin, N., Holroyd, S., Hornsby, T., Jagels, K., Krogh, A., McLean, J., Moule, S., Murphy, L., Oliver, K., Osborne, J., Quail, M. A., Rajandream, M. A., Rogers, J., Rutter, S., Seeger, K., Skelton, J., Squares, R., Squares, S., Sulston, J. E., Taylor, K., Whitehead, S., and Barrell, B. G. (1998) *Nature 393*, 537−544.
49. Deckert, G., Warren, P. V., Gaasterland, T., Young, W. G., Lenox, A. L., Graham, D. E., Overbeek, R., Snead, M. A., Keller, M., Aujay, M., Huber, R., Feldman, R. A., Short, J. M., Olsen, G. J., and Swanson, R. V. (1998) *Nature 392*, 353−358.
50. Kawarabayasi, Y., Sawada, M., Horikawa, H., Haikawa, Y., Hino, Y., Yamamoto, S., Sekine, M., Baba, S., Kosugi, H., Hosoyama, A., Nagai, Y., Sakai, M., Ogura, K., Otsuka, R., Nakazawa, H., Takamiya, M., Ohfuku, Y., Funahashi, T., Tanaka, T., Kudoh, Y., Yamazaki, J., Kushida, N., Oguchi, A., Aoki, K., and Kikuchi, H. (1998) *DNA Res. 5*, 147−155.
51. Klenk, H. P., Clayton, R. A., Tomb, J. F., White, O., Nelson, K. E., Ketchum, K. A., Dodson, R. J., Gwinn, M., Hickey, E. K., Peterson, J. D., Richardson, D. L., Kerlavage, A. R., Graham, D. E., Kyrpides, N. C., Fleischmann, R. D., Quackenbush, J., Lee, N. H., Sutton, G. G., Gill, S., Kirkness, E. F., Dougherty, B. A., McKenney, K., Adams, M. D., Loftus, B., Peterson, S., Reich, C. I., McNeil, L. K., Badger, J. H., Glodek, A., Zhou, L. X., Overbeek, R., Gocayne, J. D., Weidman, J. F., McDonald, L., Utterback, T., Cotton, M. D., Spriggs, T., Artiach, P., Kaine, B. P., Sykes, S. M., Sadow, P. W., DAndrea, K. P., Bowman, C., Fujii, C., Garland, S. A., Mason, T. M., Olsen, G. J., Fraser, C. M., Smith, H. O., Woese, C. R., and Venter, J. C. (1997) *Nature 390*, 364−370.
52. Smith, D. R., Doucette-Stamm, L. A., Deloughery, C., Lee, H., Dubois, J., Aldredge, T., Bashirzadeh, R., Blakely, D., Cook, R., Gilbert, K., Harrison, D., Hoang, L., Keagle, P., Lumm, W., Pothier, B., Qiu, D., Spadafora, R., Vicaire, R., Wang, Y., Wierzbowski, J., Gibson, R., Jiwani, N., Caruso, A., Bush, D., Safer, H., Patwell, D., Prabhakar, S., McDougall, S., Shimer, G., Goyal, A., Pietrokovski, S., Church, G. M., Daniels, C. J., Mao, J. I., Rice, P., Nolling, J., and Reeve, J. N. (1997) *J. Bacteriol. 179*, 7135−7155.

BI990638R